VOL. 5, NO. 6, JUNE 2010 ISSN 1819-6608
ARPN Journal of Engineering and Applied Sciences
©2006-2010 Asian Research Publishing Network (ARPN). All rights reserved.
www.arpnjournals.com

# EXPERIMENTAL AND NUMERICAL EVALUATION OF FRICTION STIR WELDS OF AA6061-T6 ALUMINIUM ALLOY

P. Prasanna[1], B. Subba Rao[2], G. Krishna Mohana Rao[1]
[1]Department of Mechanical Engineering, JNTUH College of Engineering, Hyderabad, India
[2]Department of Mechanical Engineering, Vasavi College of Engineering, Hyderabad, India
E-Mail: kmrgurram@rediffmail.com

**ABSTRACT**

Friction stir welding is a relatively new joining process, which involves the joining of metals without fusion or filler materials. The amount of the heat conducted into the work piece dictates a successful process which is defined by the quality, shape and microstructure of the processed zone, as well as the residual stress and the distortion of the work piece. The amount of the heat gone to the tool dictates the life of the tool and the capability of the tool to produce a good processed zone. Hence, understanding the heat transfer aspect of the friction stir welding is extremely important for improving the process. Many research works were carried out to simulate the friction stir welding using various soft wares to determine the temperature distribution for a given set of welding conditions. Very few attempted to determine the maximum temperature by varying the input parameters using ANSYS. The objective of this research is to develop a finite element simulation of friction stir welding of AA6061-T6 Aluminium alloy. Trend line equations are developed for thermal conductivity, specific heat and density to know the relationship of these factors with peak temperature. Tensile and hardness values for the welded specimens are found for different rotational speed and feed. Variation of temperature with input parameters is also observed. The simulation model is tested with experimental results. The results of the simulation are in good agreement with that of experimental results.

**Keywords**: friction stir welding, aluminium alloy, mechanical tests, tensile test, hardness test, temperature, trend line equations.

## 1. INTRODUCTION

In order to avoid the difficulties involved in welding of Aluminium by traditional welding methods a new technique, Friction stir welding was developed in 1991 at Cambridge, UK. It can weld all aluminum alloys, including those that cannot normally be joined by conventional fusion welding techniques such as aluminum-lithium alloys. Dissimilar aluminum alloys can also be joined.

### 1.1 Welding of aluminum alloys

In traditional or fusion welding the material must be melting and re solidified, but in case of FSW, the joint is in solid state - it never melts. Instead, the joint is created under conditions of severe plastic deformation. The big difference between FSW and fusion welding (other than the lack of melting) is the ability to manipulate peak temperatures by choice of different welding parameters. This can be achieved accurately through simulation of the process using Simulation software like ANSYS10.0 software. This will reduce the time for simulation. FSW provides the ability to manipulate the properties of the metal and tailor them for different applications, and possible to optimize tensile strength, fracture toughness, or fatigue resistance based on the particular application.

### 1.2 Friction stir welding

FSW involves the joining of metals without fusion or filler materials and is derived from conventional friction welding which enables the advantages of solid-state welding. Friction stir welding has enjoyed worldwide interest since its inception because of its advantages over traditional joining techniques. Essentially, FSW is a local thermo-mechanical metal working process with additional adiabatic heating from metal deformation that changes the local properties without influencing properties in the remainder of the structure. As mentioned later, the pin and shoulder of the tool can be modified in a number of ways to influence material flow and micro-structural evolution.

A rotating tool with pin and shoulder is inserted in the material to be treated, and traversed along the line of interest (Figure-1). During FSW, the area to be processed and the tool are moved relative to each other such that the tool traverses with overlapping passes until the entire selected area is processed to a fine grain size. The rotating tool provides a continual hot working action, plasticizing metal within a narrow zone while transporting metal from the leading face of the pin to its trailing edge. The processed zone cools without solidification, as there is no liquid and hence a defect-free re-crystallized fine grain microstructure is formed.

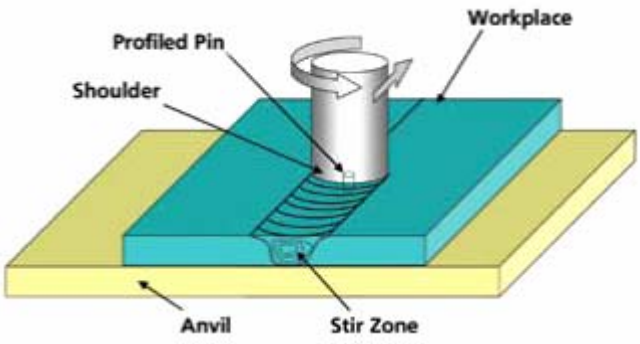


**Figure-1.** Schematic of friction stir welding.

©2006-2010 Asian Research Publishing Network (ARPN). All rights reserved.


Friction Stir welding has opened up a new process for inducing directed, localized, and controlled materials properties in any arbitrary location and pattern to achieve revolutionary capability in high value-added components. Friction stir welding provides the ability to thermo-mechanically process selective locations on the structure's surface and to some considerable depth (>25mm) to enhance specific properties. Research is being increasingly focused on this aspect of the technology for use with automotive alloys. For example, Cast aluminum alloys, such as A319, are used for suspension and drive line components in automobiles. FSW generates a fine, equi-axed grain morphology having a banded, bimodal grain size of 1 to 5 microns. The microstructure of friction stir welded aluminum alloy is normally stable under super plastic conditions of high temperature and dynamic strain. High-angle grain boundaries can enhance grain boundary sliding and related super plasticity. However, optimum super plasticity requires a homogeneous distribution of equi-axed grains of minimum grain size. Microstructures resulting from FSW do not have a uniform grain size distribution for any one set of process parameters. Grain size varies from the top to the bottom as well as from the advancing to the retreating side. The ability of friction stir welding to change the local microstructure via thermo-mechanical working has been well established by many investigators.

One of the key elements in the FSW process is the heat generated at the interface between the tool and the work piece which is the driving force to make the FSW process successful. The heat flux must be kept at maximum such that the temperature in the work piece is high enough, so that the material is sufficiently soft for the pin to stir but low enough so that the material does not melt. The maximum temperature created by FSW process ranges from 70% to 90% of the melting temperature of the work piece material, as measured by Tang *et al* (1988) and Cole grove *et al* (2000), so that welding defects and large distortion commonly associated with fusion welding are minimized or avoided. The heat flux in friction stir processing is primarily generated by the friction and the deformation process. This heat is conducted to both the tool and the work piece. The amount of the heat conducted into the work piece dictates a successful process which is defined by the quality, shape and microstructure of the processed zone, as well as the residual stress and the distortion of the work piece. The amount of the heat gone to the tool dictates the life of the tool and the capability of the tool to produce a good processed zone. For instance, insufficient heat from the friction could lead to breakage of the pin of the tool since the material is not soft enough. Therefore, understanding the heat transfer aspect of the friction stir welding is extremely important, not only for the science but also for improving the process.

### 1.3 Finite element analysis

The Basic concept of FEA is that the body or structure may be divided into smaller elements of finite dimensions called "Finite Elements". FEA can be employed effectively to perform welding simulations and to predict weld residual stresses in different types of joints and materials.

### 1.4 Aluminium alloys

Aluminum alloys are designated based on international standards. These alloys are distinguished by a four-digit number, which is followed by a temper designation code. The first digit corresponds to the principal alloying constituent(s). The second digit corresponds to variations of the initial alloy. The third and fourth digits correspond to individual alloy variations. Finally the temper designation code corresponds to different strengthening techniques. Properties of aluminum alloy AA6061 is given in Tables 1 to 3.

**Table-1.** Chemical composition AA6061-T6.

| Mg | Si | Fe | Cu | Zn | Ti | Mn | Cr | Others | Al |
|---|---|---|---|---|---|---|---|---|---|
| 0.8 -1.2 | 0.4 -0.8 | 0.7 | 0.15-0.40 | 0.25 | 0.15 | 0.15 | 0.04-0.35 | 0.05 | balance |

**Table-2.** Physical properties of AA6061.

| Physical property | Density ( $g/cm^3$ ) | Melting point (°C) | Modulus of elasticity (GPa) | Poisson ratio |
|---|---|---|---|---|
| AA6061 | 2.7 | 580 | 70-80 | 0.33 |

©2006-2010 Asian Research Publishing Network (ARPN). All rights reserved.


**Table-3.** Mechanical properties of AA6061.

| **Temp.** | **Ultimate tensile strength** (MPa) | **0.20% Proof stress** (MPa) | **Brinell hardness** | **Elongation** (%) |
|---|---|---|---|---|
| 0 | 110-152 | 65-110 | 30-33 | 14-16 |
| T1 | 180 | 95-96 | | 16 |
| T4 | 179 | 110 | | |
| T6 | 260-310 | 240-276 | 95-97 | 9-13 |

Co-efficient of thermal expansion and thermal Conductivity are (20-100°C): $23.5x10^{-6}$ m/m°C and is173 W/m.K, respectively.

## 2. REVIEW OF LITERATURE

Chao *et al* (2003) investigated the variations of heat energy and temperature produced by the FSW in both the work piece and the pin tool. All investigations showed that the FSW of Aluminum alloys yielded welds with low distortion, high quality and low cost. Consequently, better structural performance was the primary advantage of this technology's applications. In the model developed by Chao and Qi (1998), the heat generation came from the assumption of sliding friction, where Coulomb's law was used to estimate the shear or friction force at the interface. Furthermore, the pressure at the tool interface was assumed to be constant, thereby enabling a radially dependent surface heat flux distribution as a representation of the friction heat generated by the tool shoulder, but neglecting that generated by the probe surface. Frigaard *et al* (1998, 2001) developed a process model for FSW, the heat input from the tool shoulder was assumed to be the frictional heat. The coefficient of friction was continuously adjusted to keep the calculated temperature from exceeding the material melting point. In principle, the FSW process could be applied to join other alloy materials such as Steels and Titanium. But, it is well known that current tool materials used in the FSW for Aluminum are not adequate for production applications in many of the harder alloy materials. However, when adequate wear resistant tool materials become available, the benefits of the FSW may promote its rapid implementation in the production of ferrous structures and structures made from other refractory materials. Reynolds *et al* (2000) investigated the microstructures, residual stresses and strength of the friction stir welds through experimental studies of austenitic stainless steels, and also stated that to improve the welding quality for the FSW of steels, numerical modeling and simulations of transient temperature and residual stresses are valuable and necessary.

Colegrove, Shercliff (2003) used an advanced analytical estimation of the heat generation for tools with a threaded probe to estimate the heat generation distribution. The fraction of heat generated by the probe is estimated to be as high as 20%, which leads to the conclusion that the analytical estimated probe heat generation contribution is not negligible. Chen and Kovacevic (2003) developed a three-dimensional thermo-mechanical model including the mechanical action of the shoulder and the thermo-mechanical effect of the welded material for the FSW of an Al-alloy. Schmidt *et al* (2004) established an analytical model for heat generation by friction stir welding, based on different assumptions of the contact condition between the rotating tool surface and the weld piece. The material flow and heat generation were characterized by the contact conditions at the interface, and were described as sliding, sticking or partial sliding/sticking.

Zhu and Chao (2004) conducted Three-dimensional nonlinear thermal and thermo-mechanical numerical simulations using finite element analysis code - WELDSIM on 304L stainless steel. An inverse analysis method for thermal numerical simulation was developed. McClure *et al* (1998) used Rosenthal equations to calculate temperature fields in friction stir welding, and found that the existence of the thermocouples and holes containing thermocouples did not influence the temperature field. Ulysse (2002) used a three dimensional visco-plastic modeling to model friction stir welding process. Forces applied on the tool were computed for various welding and rotational speeds. Pin forces increased with increasing welding speeds, but the opposite effect was observed for increasing rotational speeds. Vijay Soundararajan *et al* (2005) developed a finite element thermo-mechanical model with mechanical tool loading considering a uniform value for contact conductance and used for predicting the stress at the work piece and backing plate interface. This pressure distribution contours are used for defining the non-uniform adaptive contact conductance used in the thermal model for predicting the thermal history in the work piece.

Buffa. G *et al* (2006) developed a continuum based FEM model for friction stir welding process, which was 3D Lagrangian implicit, coupled, and rigid-viscoplastic. The distribution of temperature and strain in heat affect zone and the weld nugget was investigated. The model correctly predicted the non-symmetric nature of FSW process, and the relationships between the tool forces and the variation in the process parameters. It was found that the effective strain distribution was non-symmetric about the weld line while the temperature profile was almost symmetric in the weld zone. Terry Dickerson *et al* (2005) calculated the transient heat losses into FSW tools. Heat loss into the tool enabled the welding efficiency to be determined. Finally the use of grooves in the tool to impede heat flow was investigated as a way of increasing

©2006-2010 Asian Research Publishing Network (ARPN). All rights reserved.


welding efficiency and also investigated that, using solid tools the steady state heat loss into the tool was about 10% of the total heat generated.

Many researches works were carried out to simulate the friction stir welding using various FEA software to determine the temperature distribution for a given set of conditions in weldments. Very few attempted to determine the optimal temperature by varying the input parameters using ANSYS.

**Objective of the present work**

The objective of the present research is to develop a finite element simulation with improved capability to predict temperature evolution in aluminum alloys and to determine the optimal weld parameters using trend line equation. Experiments have been conducted on the AA6061 Aluminum alloy in a vertical axis CNC milling machine by programming (APT). The peak temperature attained during Friction stir welding process along the direction of the weld line and the temperature perpendicular to the weld line from maximum temperature point are measured. Comparison is made between theoretical values from ANSYS and experimental values.

## 3. SIMULATION AND GENERATION OF TREND LINE EQUATIONS

Simulation of friction stir welding has been done to get an idea about the behavior of the joints obtained. Variation of maximum temperature with respect to various factors is analyzed.

### 3.1 Variation of temperature with respect to thermal conductivity

For simulating the friction stir welding process, the average values of thermal conductivity, specific heat and density of aluminum were taken as 0.14 W/mm°C, 1100 J/Kg°C and 2.77E-06 Kg/mm$^3$ respectively. To determine the peak temperature, the specific heat and density were kept constant in the simulation program and the thermal conductivity was varied from 0.140 W/mm°C to 0.024 W/mm°C. From the simulated peak temperatures using ANSYS, a trend line equation (1) was generated using Microsoft Excel. Figure-2 shows the relation between thermal conductivity and peak temperatures.

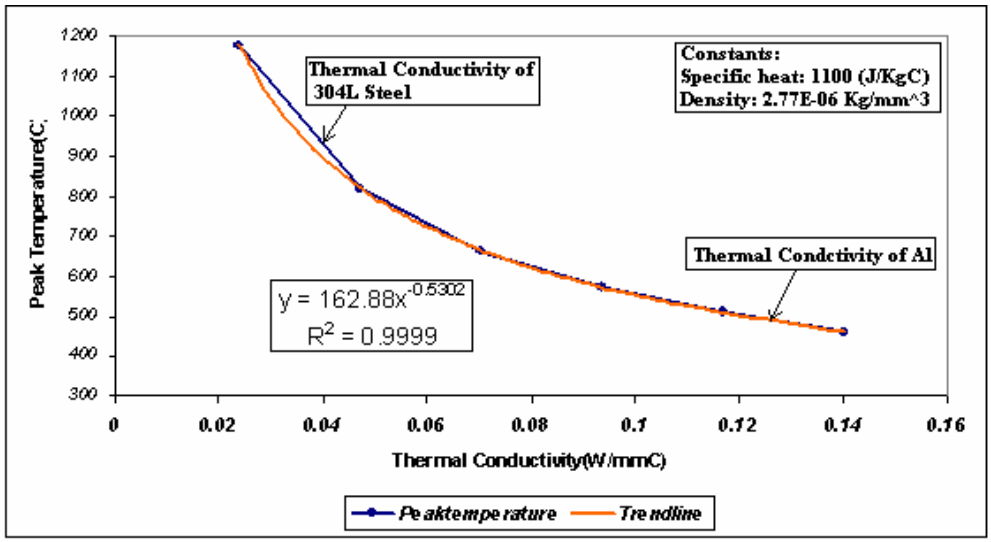


**Figure-2.** Variation in peak temperature with thermal conductivity.

The trend line equation obtained from Figure-2 is given as

$$t_1 = 162.88x^{-0.5302} \quad (1)$$

Where $t_1$ = Peak temperature, ($^o$C).
$k$ = Thermal conductivity, (W/mm$^o$C).
From the regression coefficient ($R^2$ = 0.9999), the closeness of trend line to the actual curve obtained was 99.99%.

### 3.2 Variation of temperature with respect to specific heat

For simulating the friction stir welding process, the average values of thermal conductivity, specific heat and density of aluminum were taken as 0.14 W/mm°C, 1100 J/Kg°C and 2.77E-06 Kg/mm$^3$ respectively. To determine the peak temperature, the thermal conductivity and density were kept constant in the simulation program and the specific heat was varied from 1100 J/Kg°C to 580 J/Kg°C. From the simulated peak temperatures using ANSYS, a trend line equation (2) was generated using Microsoft Excel. Figure-3 shows the relation between specific heat and peak temperatures.

©2006-2010 Asian Research Publishing Network (ARPN). All rights reserved.


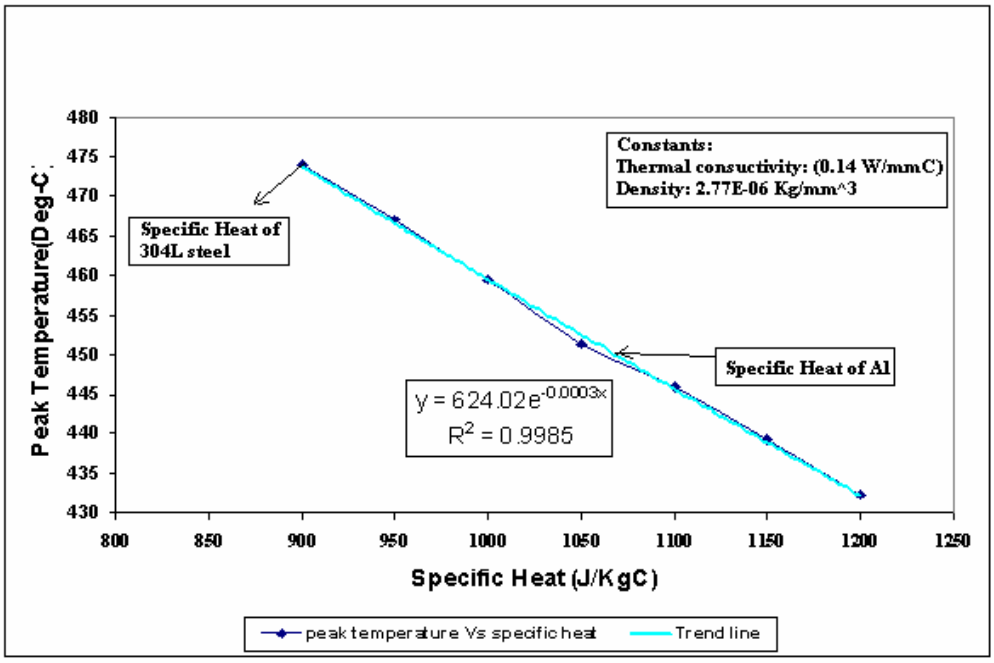


**Figure-3.** Variation in specific heat with peak temperature.

The trend line equation obtained from Figure-3 was given as

$$t_2 = 624.02e^{-0.0003x} \quad (2)$$

Where $t_2$ = Peak temperature ($^0$C).

$x$ = Specific heat (J/Kg$^0$C).

From the regression coefficient ($R^2$ = 0.9985), the closeness of trend line to the actual curve obtained was 99.85%.

### 3.3 Variation of temperature with respect to density

For simulating the friction stir welding process, the average values of thermal conductivity, specific heat and density of aluminum were taken as 0.14 W/mm°C, 1100 J/Kg°C and 2.77E-06 Kg/mm$^3$ respectively. To determine the peak temperature, the thermal conductivity and specific heat were kept constant in the simulation program and the density was varied from 2.77 E-06 Kg/mm$^3$ to 7.5E-06 Kg/mm$^3$. From the simulated peak temperatures using ANSYS, a trend line equation (3) was generated using Microsoft Excel. Figure-4 shows the relation between density and peak temperatures.

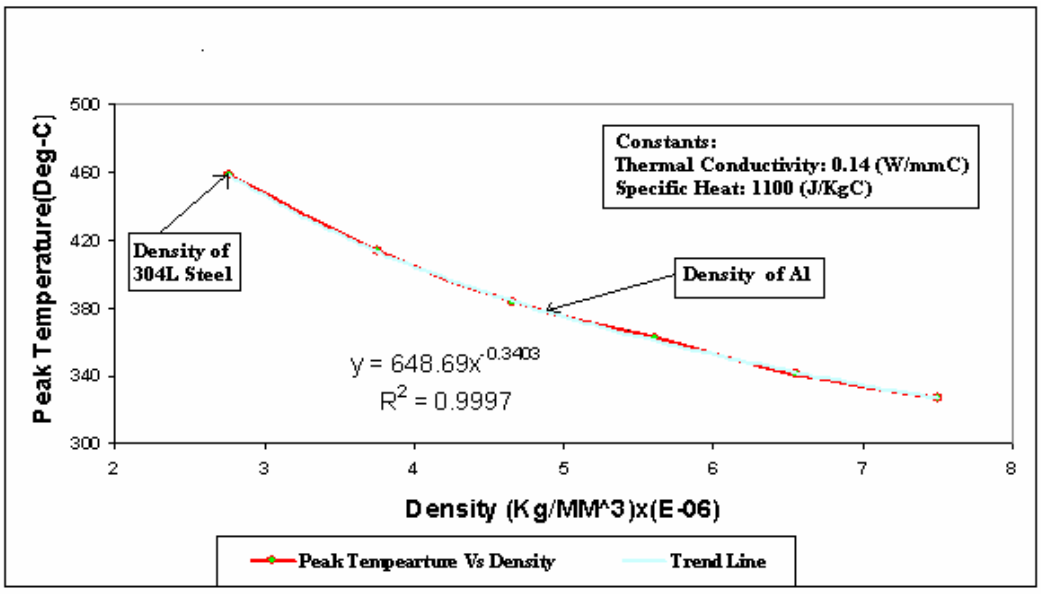


**Figure-4.** Variation in peak temperature with density.

©2006-2010 Asian Research Publishing Network (ARPN). All rights reserved.


The trend line equation obtained from Figure-4 was given as

$$t_3 = 648.69x^{-0.3403} \quad (3)$$

Where $t_3$ = Peak temperature, ($^0$C).

$x$ = Density, (Kg/mm$^3$).

From the regression coefficient ($R^2 = 0.9997$), the closeness of trend line to the actual curve obtained was 99.97%. Trend line equation for thermal conductivity variation with temperature from equation (1), was given by

$$t_1 = 162.88x^{-0.5302} \Rightarrow t_1 \propto k^{-0.5302} \quad (4)$$

Where k = thermal conductivity, (W/mm$^0$C).

Trend line equation for specific heat variation with temperature from equation (2), was given by

$$t_2 = 624.02e^{-0.0003x} \Rightarrow t_2 \propto e^{-0.0003c} \quad (5)$$

Where c = specific heat, (J/Kg$^0$C)

Trend line equation for density variation with temperature from equation (3), was given by

$$t_3 = 648.69x^{-0.3403} \Rightarrow t_3 \propto \rho^{-0.3403} \quad (6)$$

Where $\rho$ = Density, (Kg/mm$^3$)

From (4), (5), (6), the Peak temperature ($T^oC$) was given as:

$$T = z.k^{-0.5302}.e^{-0.0003c}.\rho^{-0.3403} \quad (7)$$

Where z = constant.

For aluminum, average values of thermal conductivity is k = 0.140 W/mm$^0$C, specific heat c = 1100 J/Kg$^0$C and density is $\rho = 2.77 \times 10^{-6}$ Kg/mm$^3$. The peak temperature calculated using ANSYS for aluminum with above mentioned material properties is 455$^0$ C. By substituting the above data in (7),

$$455 = z.k^{-0.5302}.e^{-0.0003c}.\rho^{-0.3403} \quad (8)$$

The z value obtained from (8) was,

$$z = 315.621 \quad (9)$$

Hence from (7) and (9), the peak temperature equation becomes:

$$T = 315.621.k^{-0.5302}.e^{-0.0003c}.\rho^{-0.3403} \quad (10)$$

For a given material, if the values of thermal conductivity, specific heat and density are known, using equation (10) the peak temperature during simulation of friction stir welding can be predicted.

FSW OF AA6061-T6

The main reason for simulating the FSW process for AA 6061 is, it is difficult to fusion weld this material especially during multiple heat repairs. Successful application of the FSW to join AA6061 will increase its applications to various structural components, particularly in the aerospace industry because of its lightweight and high strength.

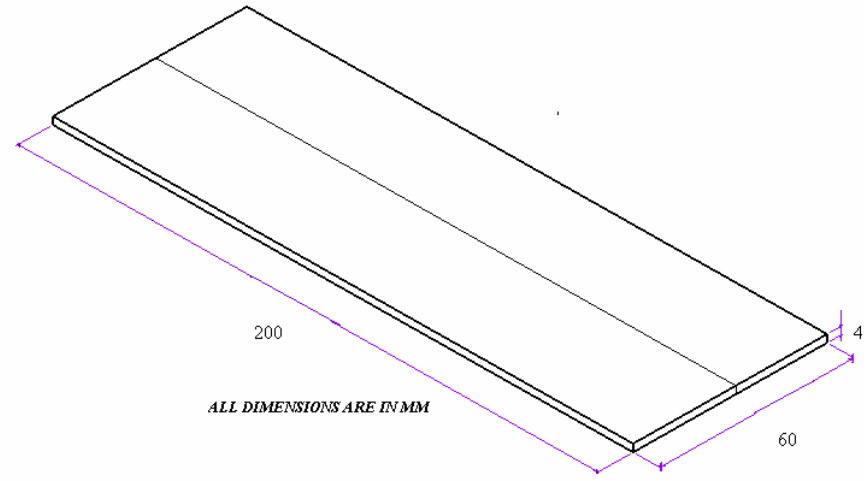


**Figure-5.** Geometry of work piece.

The work pieces having dimensions of 200 × 60 × 4 mm$^3$ as shown in Figure-5 are prepared. The tool had a shoulder radius of 10 mm, pin radius of 3.5 mm and pin length of 7 mm. A rotational speed of 250 rpm and a welding speed of 2.36 mm/sec were used for carrying out the simulation. The material properties of AA6061 are given in Table-4 and the density of the material was 2.77E-06 kg/mm$^3$.

©2006-2010 Asian Research Publishing Network (ARPN). All rights reserved.


**Table-4.** Temperature dependent material properties for AA6061-T6.

| # | **Temperature** ($^0$C) | **Thermal conductivity** (W/m$^0$C) | **Specific heat** (J/kg$^0$C) |
|---|---|---|---|
| 1 | 0 | 154 | 905 |
| 2 | 50 | 157 | 942 |
| 3 | 100 | 164 | 970 |
| 4 | 150 | 170 | 1010 |
| 5 | 200 | 176 | 1030 |
| 6 | 250 | 178 | 1060 |
| 7 | 300 | 180 | 1090 |

In the numerical simulation of the FSW of aluminum alloy, it was assumed that two plates were square butt welded. As the weld line was the symmetrical line, only one half of the work piece (200 × 60 × 4 mm$^3$) was modeled using commercial finite element package ANSYS. The finite element mesh was shown in Figure-6 which has 4 layers of elements in thickness direction and 34160 eight nodded brick elements and 35496 nodes in the analysis. At all the surfaces except at the bottom a convective heat transfer of 30 W/m$^2$ °C was used for natural convection between Aluminum and air. In friction stir welding the work pieces were clamped over back plates. A higher convective coefficient of 350 W/m$^2$ °C is applied as a boundary condition to the bottom surface of the work piece.

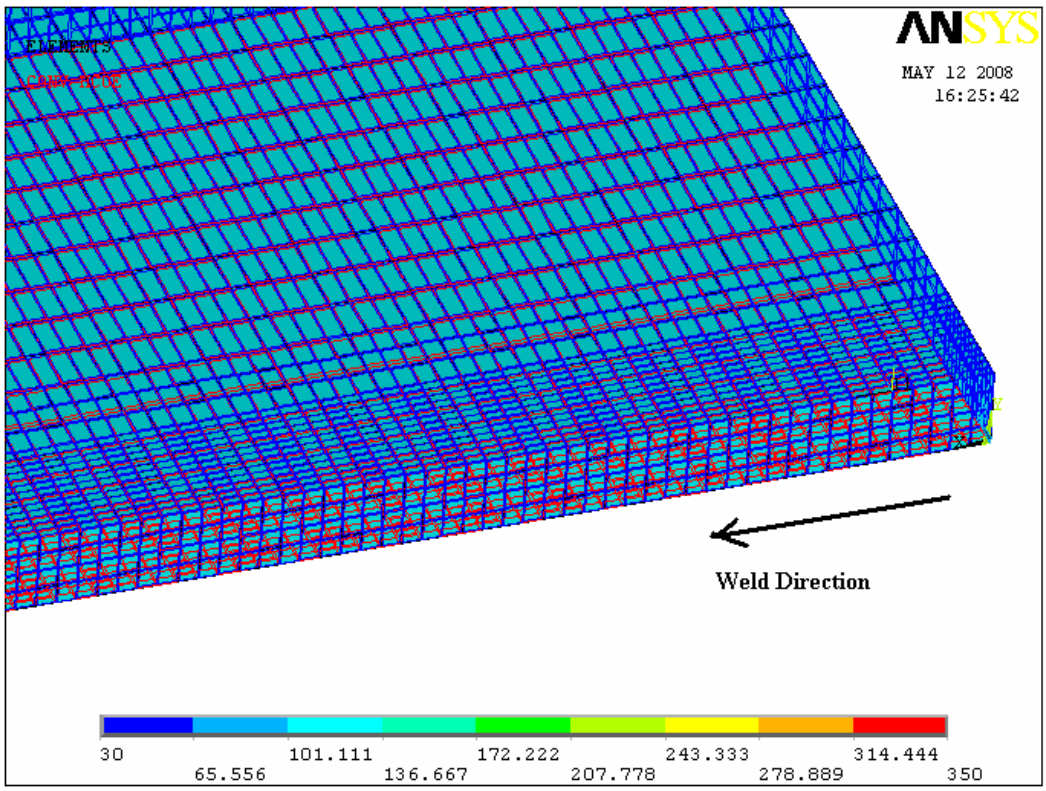


**Figure-6.** Meshed model of the work piece with loading conditions.

The model shown in Figure-6 was simulated for 290 load steps by applying appropriate boundary conditions and thermal loads. The results obtained are discussed in the next chapter.

## 4. EXPERIMENTAL DETAILS

Experimental work is done on the material selected choosing important input parameters.

### 4.1 Experimental setup

The FSW was carried out on 3-axis CIMTRIX make computer numerical controlled milling machine with FANUC controller. Computer Numerical Control milling machine is the most common form of CNC. CNC mills can perform the functions of drilling and often turning. CNC mills are classified according to the number of axes that they posses and these axes are labeled as X and Y for horizontal moment, and Z for vertical movement. CNC milling machines are traditionally programmed using a set of commands known as G codes represent specific CNC

©2006-2010 Asian Research Publishing Network (ARPN). All rights reserved.


functions in Alpha numeric format. The milling machine used in the present study is shown in Figure-7 and its specification is given in Table-5.

**Figure-7.** 3-Axis CIMTRIX CNC milling machine.

**Table-5.** CNC milling machine specifications.

| S. No. | Part name | Specifications |
|---|---|---|
| 1 | 3-axis machine center | Spinner |
| 2 | Model | BME45 |
| 3 | Spindle driver | Servo motor |
| 4 | Spindle range | 10-6000 rpm |
| 5 | Tool holder | ISO40 |
| 6 | Cutting fluid | Nr |
| 7 | Tool | HSS |
| 8 | Work piece | AA6351 |
| 9 | Movement | 610*450 |
| 10 | Bed size | 800*500 |

### 4.2 Friction stir welding equipment

In friction stir welding process fixtures are used to support the work pieces and clamp tightly and the arrangement is shown in Figure-8.

**Figure-8.** Fixture used in FSW.

A rotating tool will generate the heat between the tool and work piece, joining of two pieces together. In FSW Tool is the main element and is shown in the Figure-9.

©2006-2010 Asian Research Publishing Network (ARPN). All rights reserved.


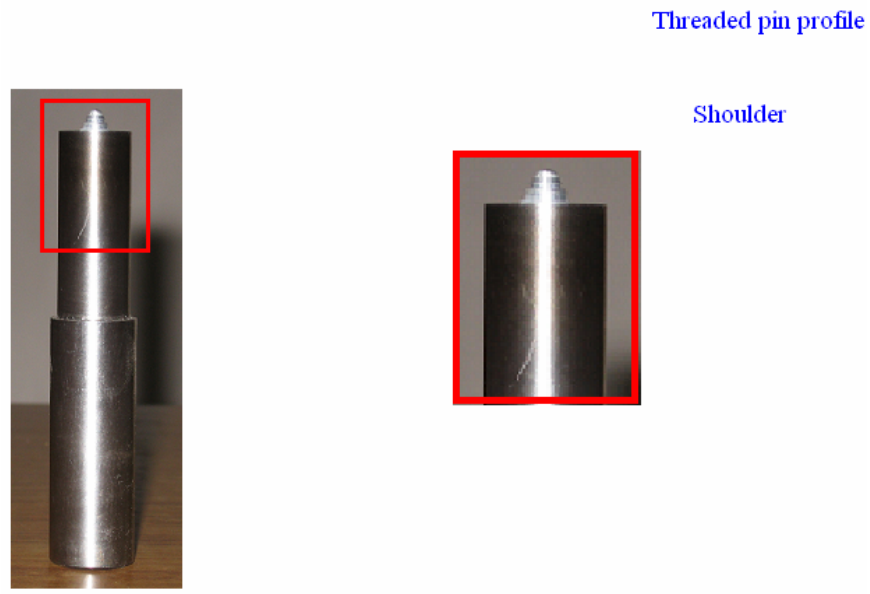


**Figure-9.** Tool used in friction stir welding.

### 4.3 Experimental plan

During the experimental process eight work pieces of dimension (200X60X4) mm are taken for joining process .Four joints are obtained from eight work pieces and the details are given in Table-6.

**Table-6.** Experimental plan.

| **Joint No** | **Rotational speed** (rpm) | **Feed** (mm/min) | **Welding position** |
|---|---|---|---|
| 1 | 850 | 16 | Forward welding |
| 2 | 950 | 16 | Reverse welding |
| 3 | 950 | 16 | Forward welding |
| 4 | 950 | 16 | Reverse welding |

A milling machine was used for friction stir welding (FSW) of Aluminum alloy. The machine is having a maximum speed of 6000 rpm and 10-horse power. The experiments were conducted on the Aluminum alloy 6061. Before the friction welding, the weld surface of the base material was cleaned. The rotating pin was inserted into an initially predrilled hole of 4.5mm long Tool tilt angle was $2^{o}$. Welding was initiated at spindle speed of 850 rpm and travel rate of 16mm/min. The speed was increased by 50rpm every pass up to a final speed of 950rpm. The same step was repeated for forward and reverse directions.

In the present work temperature distribution in work piece is measured by using Resistance Temperature Detector (RTD) as shown in Figure-10. RTD sensing element consists of a wire coil or deposited film of pure metal. The element's resistance increases with temperature in a known and repeatable manner. RTD's exhibit excellent accuracy over a wide temperature range and represent the fastest growing segment among industrial temperature sensor. RTD's can measure temperatures from -200°C to 650°C.

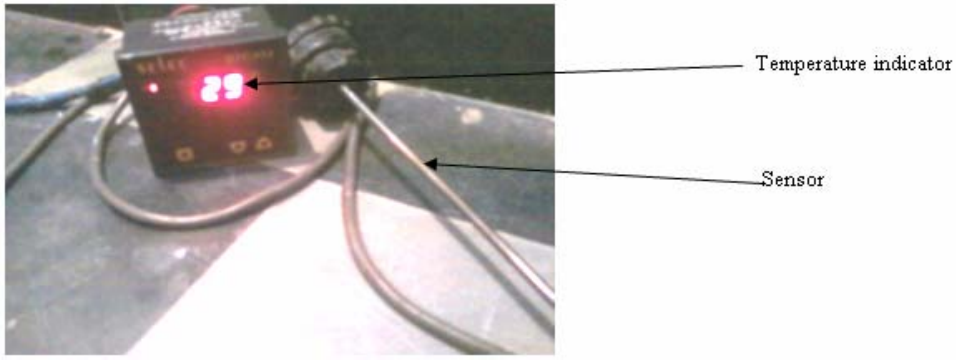


**Figure-10.** Resistance temperature detector.

©2006-2010 Asian Research Publishing Network (ARPN). All rights reserved.


In friction stir welding process heat is generated at the contact between rotating tool and work piece that plasticizes the material of work piece under it. The temperature distribution in work piece is very important as it affects the thermal stresses developed in FSW process. In the present work temperature is measured made by placing a sensor at different points on the work piece along the direction of weld line and also perpendicular to it. Temperature is measured using an RTD and the physical arrangement is shown in Figure-11.


**Figure-11.** Measurement of temperature by using resistance temperature detector.

The hardness test gives an idea of the resistance to indentation of the weld metal. This is important with respect to components which have been built up and have to withstand abrasive wear. Hardness values can give information about the metallurgical changes caused by welding. Brinell hardness test is conducted on the second joint at different points on the weld zone along the direction of weld line. The hardness is tested for parent material as it is expected that hardness variation on the material surface is inherent and is influenced by a number of metallurgical parameters during solidification of the material. The hardness is also tested along the weld seam at four points from a reference point.

The Tensile test is conducted on the AA 6061 friction stir welded joints in a Universal Testing Machine as per ASTM standards to determine the breaking load and yield strength of the weldment. Three pieces cut from second joint of dimension (20.10X4.00) mm are tested on Universal Testing Machine. Tensile test specimens are shown in Figure-12.

a) First work piece from 50$^{o}$C -90$^{o}$C temperature region.
b) Second work piece from 260oC -240oC temperature region.
c) Third work piece from 280 oC-420oC temperature region.

**Figure-12.** Specimen preparation before tensile test.

## 5. RESULTS AND DISCUSSIONS

The experimented details of friction stir welding process for AA6061-T6 material was explained in previous chapter .The results obtained in experimental process are discussed below. Temperature distribution on the surface of the specimens is measured for different rotational speeds.

Table-7 gives the temperature values for the first joint in a direction perpendicular to the direction of weld at a rotational speed of 850 rpm in forward direction. It is observed that the maximum temperature is 400$^{0}$C occurring at the center of welding zone which is slowly reducing for farther points. Similar phenomenon can be observed for other rotational speeds and welding directions and the data is presented in Tables 8 to 10.

**Table-7.** Temperature values for first joint perpendicular to the direction of weld line from maximum temperature point at rotational speed of 850 rpm and feed of 16mm/min in reverse direction.

| S. No. | **Distance** (cm) | **Temperature** ($^{0}$C) |
|---|---|---|
| 1 | 0 | 400 |
| 2 | 0.8 | 260 |
| 3 | 1.6 | 170 |
| 4 | 2.4 | 140 |

©2006-2010 Asian Research Publishing Network (ARPN). All rights reserved.


**Table-8.** Temperature values for second joint perpendicular to the direction of weld line from maximum Temperature point at rotational speed of 950 rpm and feed of 16mm/min in reverse direction.

| S. No. | Distance (cm) | Temperature ($^0$C) |
|---|---|---|
| 1 | 0 | 420 |
| 2 | 0.8 | 280 |
| 3 | 1.6 | 190 |
| 4 | 2.4 | 160 |

**Table-9.** Temperature values for third joint perpendicular to the direction of weld line from maximum temperature point at rotational speed of 950 rpm and feed of 16mm/min in forward direction.

| S. No. | Distance (cm) | Temperature ($^0$C) |
|---|---|---|
| 1 | 0 | 406 |
| 2 | 0.8 | 270 |
| 3 | 1.6 | 180 |
| 4 | 2.4 | 150 |

**Table-10.** Temperature values for fourth joint perpendicular to the direction of the weld line from maximum temperature point at rotational speed of 950 rpm and feed of 16mm/min in reverse direction.

| S. No. | Distance (cm) | Temperature ($^0$C) |
|---|---|---|
| 1 | 0 | 410 |
| 2 | 0.8 | 275 |
| 3 | 1.6 | 185 |
| 4 | 2.4 | 155 |

The tensile test is conducted on three specimens and the values of tensile strength obtained are given in Table-11.

**Table-11.** Tensile test results.

| Work piece number | Width X thick (mm) | Yield load (kN) | Tensile strength (N/mm$^2$) |
|---|---|---|---|
| 1 | 20.10X4.00 | 1.50 | 18.66 |
| 2 | 20.09X4.00 | 1.70 | 21.15 |
| 3 | 20.07X4.00 | 2.80 | 34.88 |

Figure-13 shows the variation in temperature with distance on the top surface for four joints in forward direction and reverse direction of the weld. The peak temperature obtained was 420$^0$ C in second joint in reverse direction of weld. From Figure-13 it can be observed that the maximum temperature obtained in reverse direction of the weld and maximum temperature obtained for second joint is 70% of the melting point temperature of the AA6061-T6 which indicates that the quality of weld obtained is good. The Brinell's Hardness number observed during friction stir welding of AA 6061 in reverse welding processes on second joint because the peak temperature obtained in friction stir welding process is 70% of the melting point temperature. Hardness variation on the material surface is inherent and is influenced by a number of metallurgical parameters during solidification of the material.

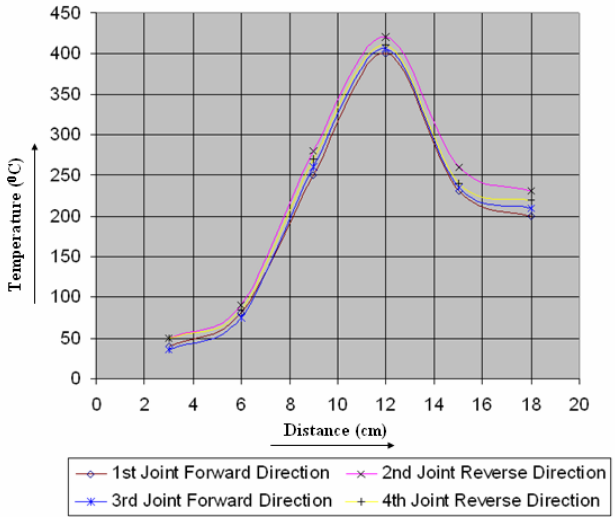


**Figure-13.** Variation in temperature with distance along the weld line on the top surface.

Figure-14 shows the Variation of Brinell's hardness number across the weld zone. It can be observed that the brinell's hardness number first increases and then decreases across the weld zone. Higher hardness value occurred at maximum temperature point due to the formation of new grains. The Tensile test is conducted on the AA 6061 friction stir elements in a Universal Testing Machine as per ASTM standards to determine the breaking load and yield strength of the weldment. From tensile test maximum tensile strength is obtained in the maximum temperature region. The simulation of friction stir welding process for AA6061-T6 material is already explained. The results obtained through the simulation process for different input parameters are discussed below.

**Variation of temperature with respect to rotational and welding speeds**

Figure-15 shows the variation of temperature for different rotational speeds with distance, at constant welding speed of 2.36 mm/s.

©2006-2010 Asian Research Publishing Network (ARPN). All rights reserved.


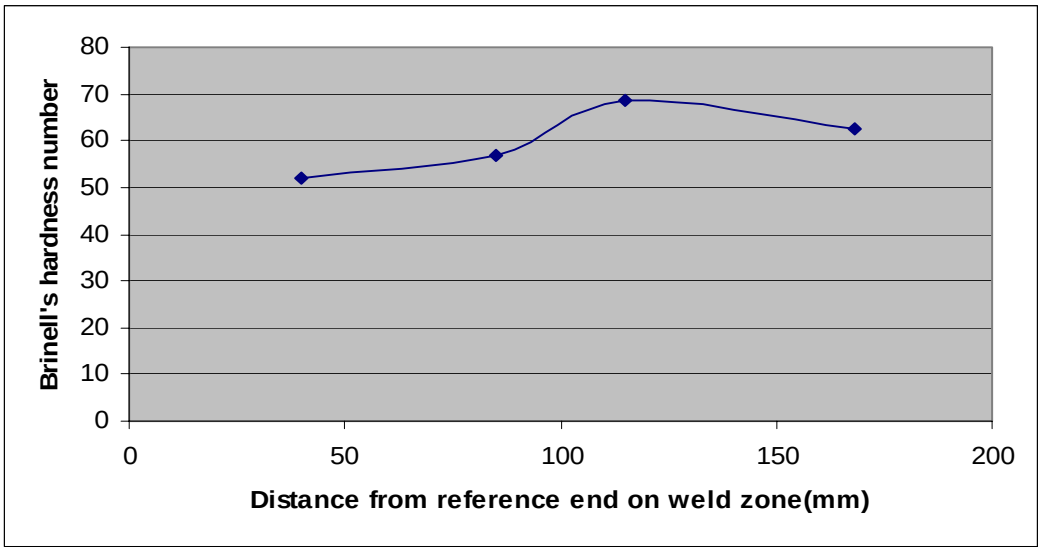


**Figure-14.** Variation of Brinell's hardness number with distance along the weld zone.

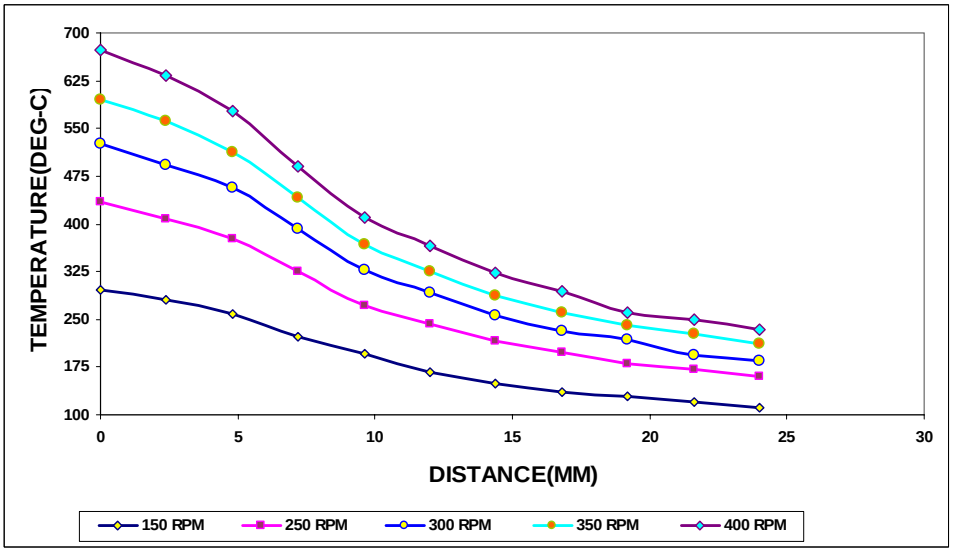


**Figure-15.** Variation of temperature with distance on top surface with varying rotational speeds.

Figure-16 shows variation in temperature with time at different rotational speeds, and at constant welding speed. For all rotational speeds the maximum temperature occurred at 16.5seconds.

©2006-2010 Asian Research Publishing Network (ARPN). All rights reserved.


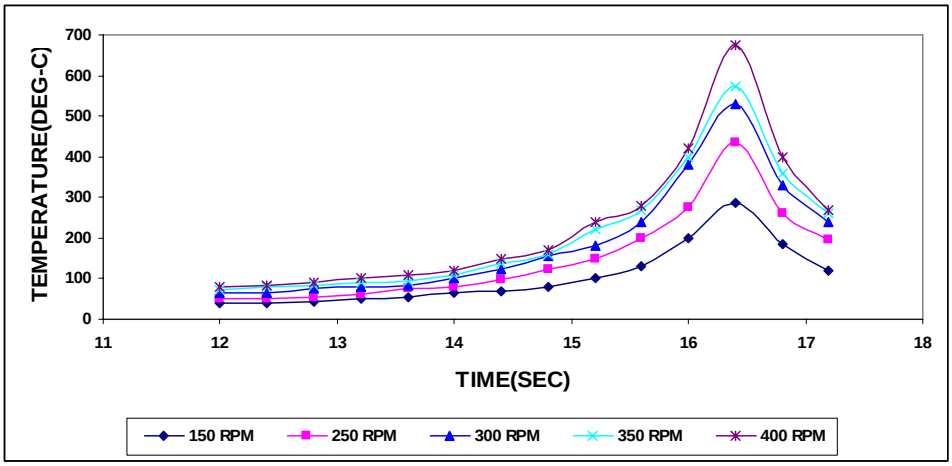


**Figure-16.** Variation in temperature with time on the top surface.

Figure-17 shows temperature variation with distance for different welding speeds, at constant rotational speed of 250 rpm.

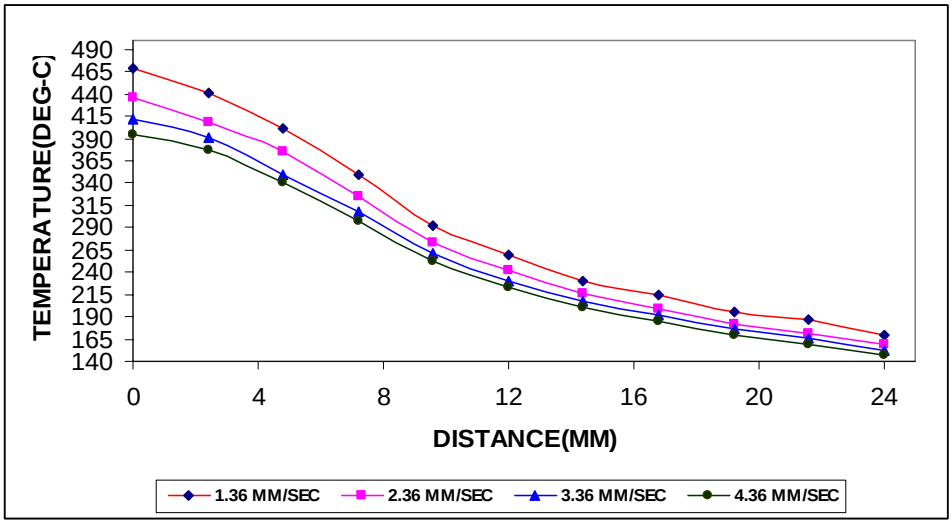


**Figure-17.** Variation of temperature on the top surface, with varying welding speeds.

It is evident from Figure-16 that keeping the applied force and welding speed constant, as the rotational speed increases the peak temperature increases. However to attain a good processed zone the optimum operating temperature for material Al6061 is between $420^0$C and $450^0$C. As the coefficient of friction and radius of the shoulder and pin are constant for the current investigation, the increase in rotational speed has to be compensated by decreasing the applied force. Similarly, as the welding speed increases, the contact time per unit area of tool - work piece interface is reduced thus reducing the peak temperature.

The predicted peak temperature for AA6061 alloy using the trend line equation (10) is 438°C, and the obtained peak temperature from ANSYS is $435.439^0$C. This shows the peak temperature obtained at the input parameters of 250 rpm and 2.36 mm/s was close to the result obtained from ANSYS. Figure-18 shows the variation in temperature with distance along the top surface perpendicular to the weld line at node-37634 (82, 8, 0). The peak temperature obtained is $435.439^0$C. This is about 75% of melting point temperature of the work piece ($580^0$C). So the quality of the weld was good according to Tang *et al* [1]. Figure-19 shows the variation in temperature with distance along the top surface perpendicular to the weld line on the top surface for different joints (experimental) and theoretical model from ANSYS. From Figure-18 temperature decreases with distance along the top surface perpendicular to the weld line. From experiments peak temperature obtained is $420^0$C and this temperature is nearer to the theoretical value from ANSYS.

©2006-2010 Asian Research Publishing Network (ARPN). All rights reserved.


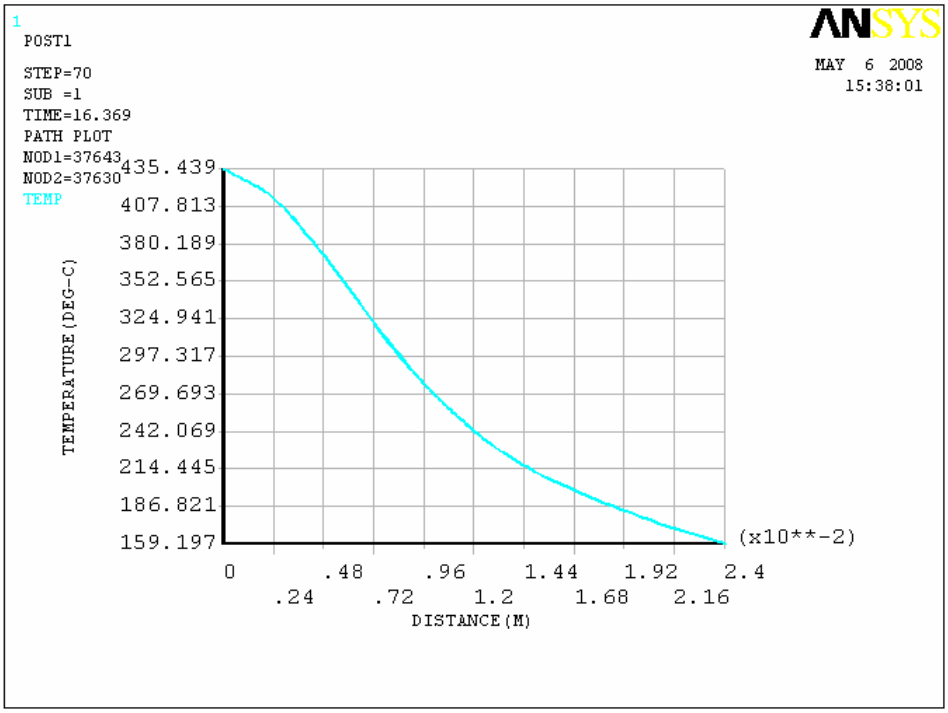


**Figure-18.** Variation in temperature with distance along the line perpendicular to the weld line on the top surface at node-37643 (82, 8, 0).

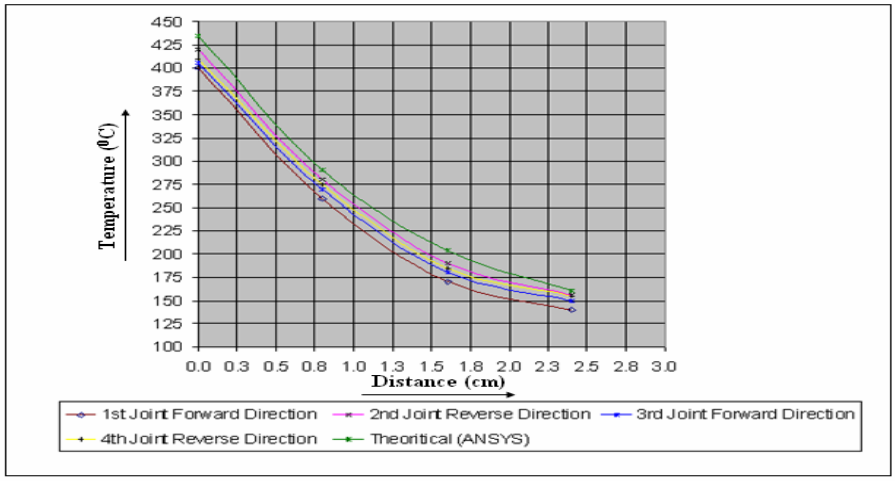


**Figure-19.** Variation in temperature with distance along the perpendicular to the weld line on the top surface for different joints and theoretical model from ANSYS.

Figure-20 shows the variation in peak temperature with time along the weld line on top surface. From Figure-20 temperature increases and then decreases with time along the weld line. Figure-21 shows the nodal temperature distribution on the work piece at node - 37643 (82, 8, 0). From Figure-20 minimum temperature obtained is $25^0$C. Figure-22 Shows variation in temperature with distance at the node 19895, which is at (82, 4, 0) from origin. From Figure-22 temperature decreases with distance perpendicular to the weld line on top surface. Figure-23 shows the variation in peak temperature with distance along the node. Figure-24 shows the temperature distribution at a time of 10 sec, the peak temperature obtained is $437.253^0$C. Figure-25 shows the temperature distribution at a time of 15 sec, the peak temperature obtained is $437.253^0$C.

©2006-2010 Asian Research Publishing Network (ARPN). All rights reserved.


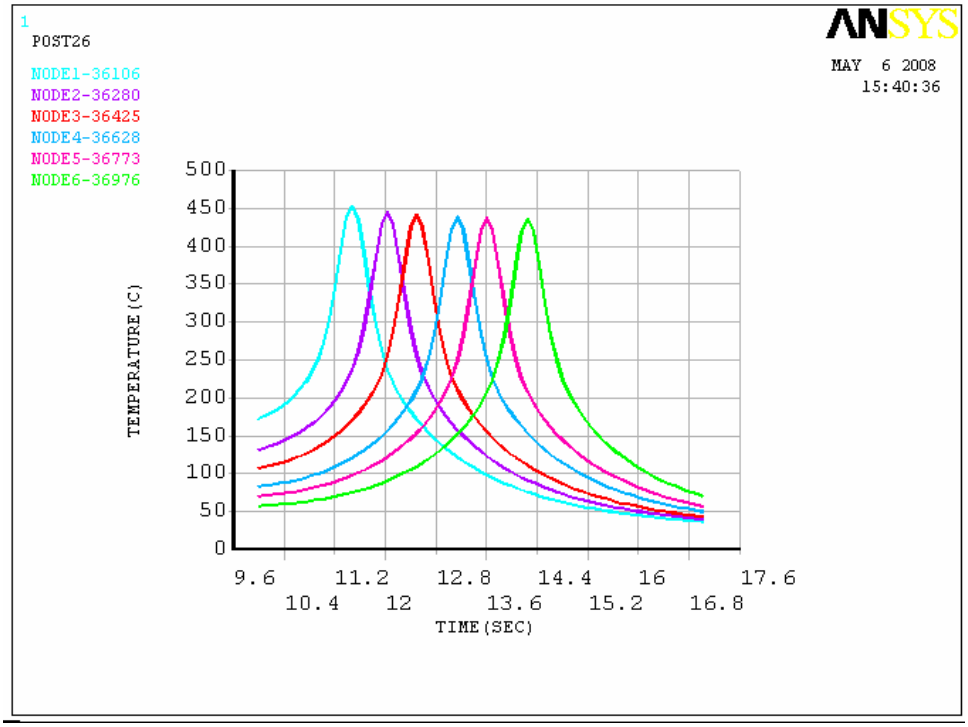


**Figure-20.**Variation in temperature with time along the weld line.

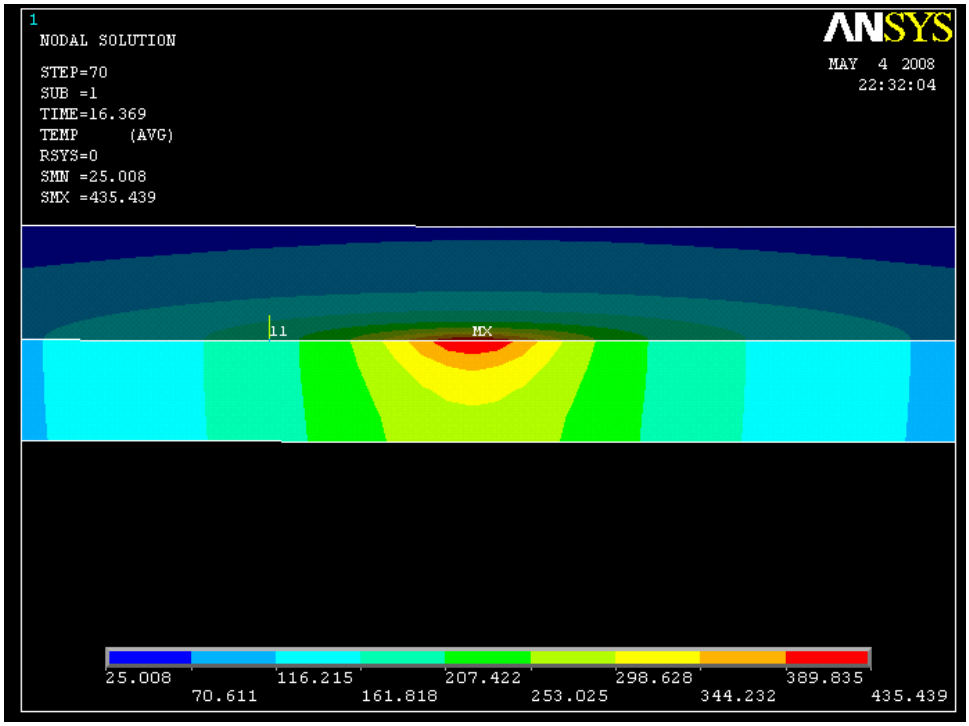


**Figure-21.** Nodal temperature along the work piece at node-37643 (82, 8, 0).

©2006-2010 Asian Research Publishing Network (ARPN). All rights reserved.


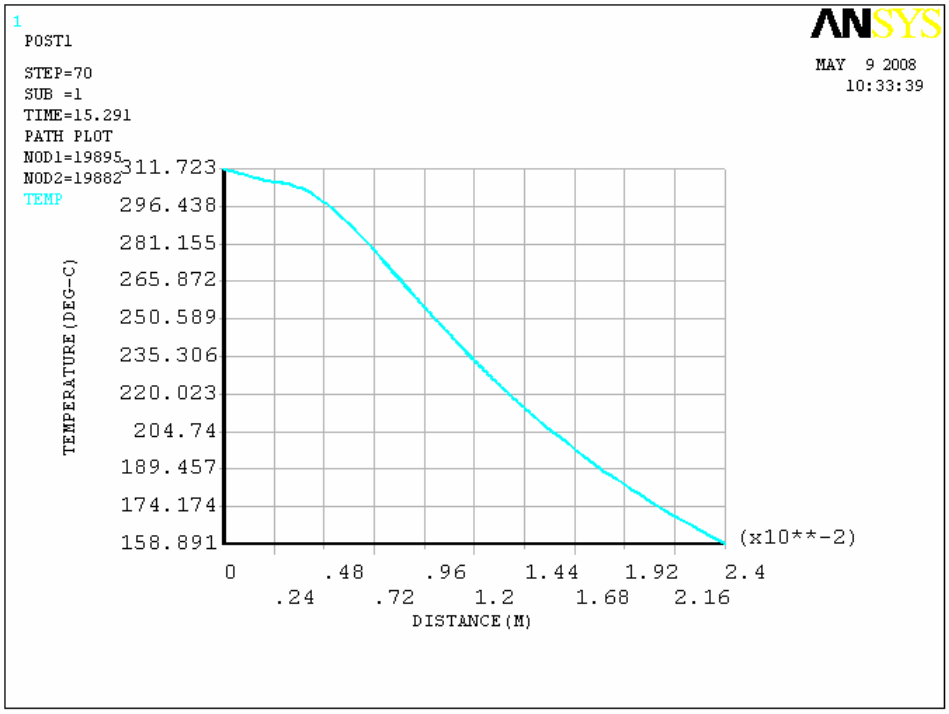


**Figure-22.** Variation in temperature with distance at node -19895(82, 4, 0).

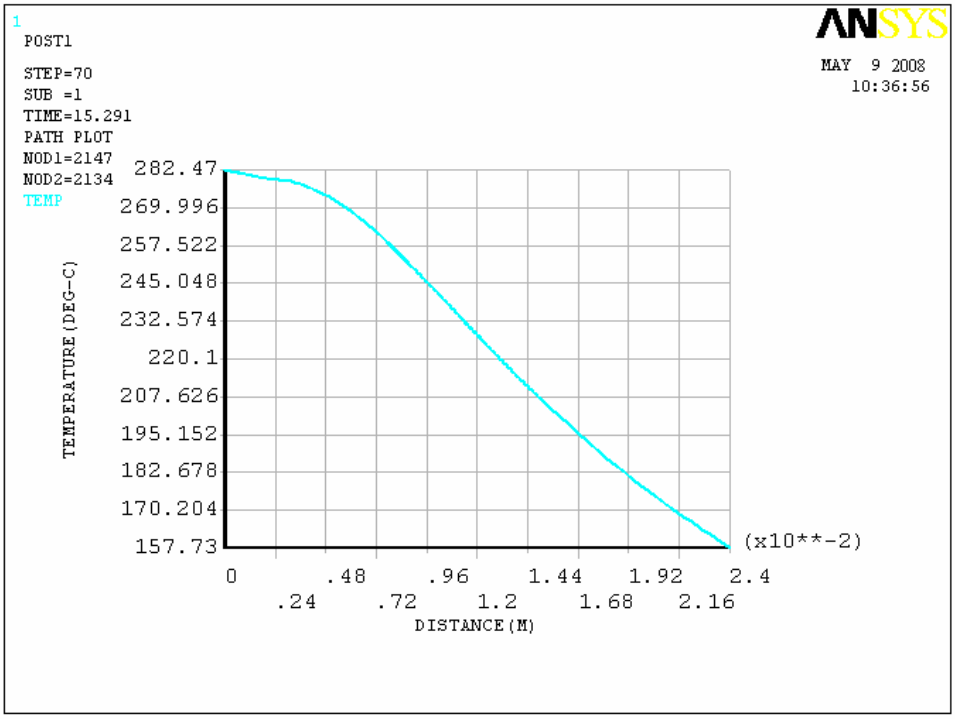


**Figure-23.** Variation in temperature with distance at node 2147 (82, 0, 0).

©2006-2010 Asian Research Publishing Network (ARPN). All rights reserved.


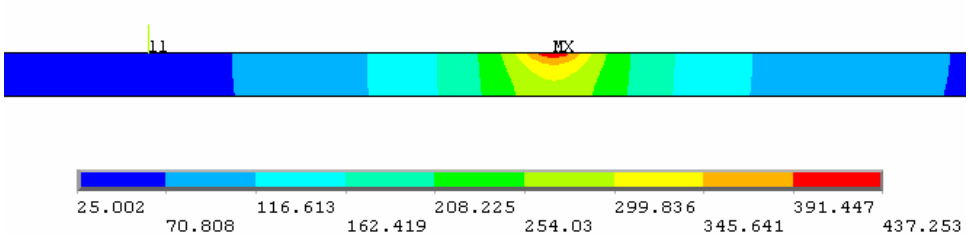


**Figure-24.** Calculated isotherms in FSW of AA6061-T6 at t = 10sec.

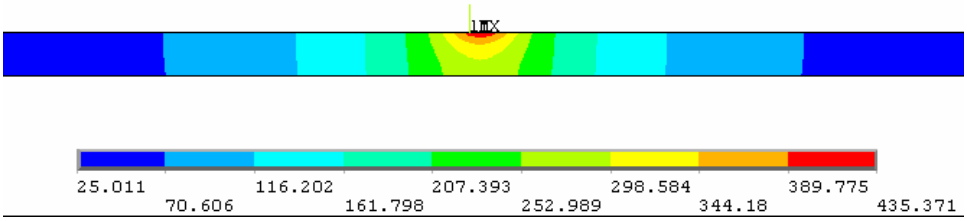


**Figure-25.** Calculated isotherms in FSW of AA6061-T6 at t = 15sec.

## 6. CONCLUSIONS

A three dimensional thermal model is developed for simulating the heat transfer process for friction stir welding of AA6061-T6 alloy, by using APDL programming code in ANSY.

- The variation in peak temperature perpendicular to the weld line at different rotational speeds and welding speeds.
- Variation of the nugget-zone temperature with respect to time
- The temperature decreases with distance perpendicular direction of the tool on the top surface for varying rotational speeds at constant welding speed.
- The temperature increases with time on the top surface for different rotational speeds at constant welding speed.
- The temperature decreases with distance on the top surface for varying welding speed at constant rotational speed.
- The variation of peak temperature with respect to thermal conductivity, specific heat and density is obtained.
- It is found that the moving heat source technique was reliable to simulate the friction stir welding process
- A trend line equation is developed to predict the peak temperature attained during friction stir welding process. Though the average values of material properties are used for simulation, the simulated results obtained from FEA are not significantly affected.
- Experiments are conducted on AA6061 Aluminum alloy in a Vertical axis CNC milling machine by programming. Brinell hardness test is conducted on AA 6061 friction stir welded joint. Tensile test is conducted on the AA6061 Friction stir welded joints in a universal tensile testing machine.
- The temperature decreases with distance in a direction perpendicular to the tool on the top surface for varying rotational speeds at constant welding speed.
- From Brinell hardness test higher hardness value is obtained at maximum temperature point.
- From tensile test maximum tensile strength is obtained in maximum temperature region.
- Comparison of temperature profile developed between theoretical values and the experimental results showed the possibility of more accurate determination using present model.
- Optimal temperature values are determined by varying input parameters. The obtained temperature is about 70 to 90% of melting point temperature of work piece material. This indicated that the quality of the weld is good. From the trend line equation it is proved that this technique can be used to various types of Aluminum alloys.

## REFERENCES

Buffa G., Huaa J., Shivpuri R., Fratini L. 2006. A continuum based fem model for friction stir welding-model development. Journal of material science and engineering. A419. pp. 389-396.

Chao Y.J. and Qi X. 1998. Thermal and Thermomechanical Analysis of Friction Stir Joining of AA6061-T6. Journal of Mat. Process and Manufac. Sci. pp. 215-233.

Chao Y.J., Qi X., Tang W. 2003. Heat Transfer in Friction Stir Welding-Experimental and Numerical Studies. ASME J. Manuf. Sci. and Engg. 25: 138-145.

Chen C.M., Kovacevic R. 2003. Finite Element Modeling of Friction Stir Welding-Thermal and Thermo-Mechanical Analysis. International Journal of Machine Tools and Manufacture. 43: 1319-1326.

©2006-2010 Asian Research Publishing Network (ARPN). All rights reserved.



Colegrove P., Painter M., Graham D. and Miller T. 2000. 3 Dimensional Flow and Thermal Modeling of the Friction Stir Welding Process. Proceedings of the Second International Symposium on Friction Stir Welding, Gothenburg, Sweden.

Colegrove P. A. and Shercliff H. R. 2003. Experimental and Numerical Analysis of Aluminium Alloy 7075-T7351 Friction Stir Welds. Science and Technology of Welding and Joining. 8, 5, IoM Communications Ltd. pp. 360-368.

Frigaard Grong, Midling O.T. 1998. Modeling of the Heat Flow Phenomena in Friction Stir Welding of Aluminum Alloys. Proceedings of the Seventh International Conference Joints in Aluminum-INALCO '98, Cambridge, UK, April 15-17. pp. 1189-1200.

Frigaard Grong, Midling O.T. 2001. A Process Model for Friction Stir Welding of Age Hardening Aluminum Alloys. Metallurgical and Materials Transactions A, Physical Metallurgy and Materials Science. Vol. 32A, No. 5, May, ASM International. pp. 1189-2000.

McClure J.C., Tang W., Murr L.E., Guo X., Feng Z., Gould J.E. 1998. A Thermal Model of Friction Stir Welding. International Conference on Trends in Welding Research. 349: 156-165.

Reynolds A.P., Lockwood W.D., Seidel T.U. 2000. Processing - Property Correlation in Friction Stir Welds. Material Science Forum. 331-337. pp. 1719-1724.

Schmidt H., Hattel J. and Wert J. 2004. An Analytical Model for the Heat Generation in Friction Stir Welding. Modeling and Simulation in Material Science Engineering. 12: 143-157.

Tang W., Guo X., McClure J.C., Murr L.E., Nunes A. 1988. Heat Input and Temperature Distribution in Friction Stir Welding. Journal of Mat. Process. and Manufg. Sci. 5: 163-172.

Terry Dickerson, Qing-yu Shi, Hugh R Shercliff. 2003. Heat Flow into Friction Stir Welding Tools. Proceedings of 4th international symposium on friction sitr welding, USA. pp. 14-16.

Ulysse P. 2002. Three Dimensional Modeling of Friction Stir Welding Process. International Journal of Machine Tools and Manufacture. 42: 1549-1557.

Vijay Soundararajan, Srdja Zekovic, Radovan Kovacevic. 2005. Thermo-mechanical model with adaptive boundary conditions for friction stir welding of Al 6061. International Journal of Machine Tools and Manufacture. 45: 1577-1587.

Zhu X.K., Chao Y.J. 2004. Numerical Simulation of Transient Temperature and Residual Stresses in Friction Stir Welding of 304L Stainless Steel. Journal of Materials Processing Technology. 146: 263-272.